INSTITUTE OF PHYSICS PUBLISHING SUPERCONDUCTOR SCIENCE AND TECHNOLOGY

Supercond. Sci. Technol. **19** (2006) S67–S83 doi:10.1088/0953-2048/19/3/010

Overview and status of the Next European Dipole Joint Research Activity

A Devred[1,2], B Baudouy[1], D E Baynham[3], T Boutboul[2], S Canfer[3], M Chorowski[4], P Fabbricatore[5], S Farinon[5], H Félice[1], P Fessia[2], J Fydrych[4], V Granata[6], M Greco[5], J Greenhalgh[3], D Leroy[2], P Loverige[3], M Matkowski[4], G Michalski[4], F Michel[1], L R Oberli[2], A den Ouden[7], D Pedrini[6], S Pietrowicz[4], J Polinski[4], V Previtali[2], L Quettier[1], D Richter[2], J M Rifflet[1], J Rochford[3], F Rondeaux[1], S Sanz[8], C Scheuerlein[2], N Schwerg[2,9], S Sgobba[2], M Sorbi[6,10], F Toral-Fernandez[8], R van Weelderen[2], P Védrine[1] and G Volpini[6]

[1] CEA/DSM/DAPNIA/SACM, 91191 Gif-sur-Yvette CEDEX, France
[2] CERN, CH-1211 Genève 23, Switzerland
[3] Engineering Department, CCLRC/RAL, Chilton, Didcot, Oxon OX11 0QX, UK
[4] Institute of Power Engineering and Fluid Mechanics, Wroclaw University of Technology, Wybrzeze Wyspianskiego 27, 50 370 Wroclaw, Poland
[5] INFN-Genova, via Dodecaneso 33, 16146 Genova, Italy
[6] INFN-Milan/LASA, via Fratelli Cervi 201, 20090 Segrate (Milan), Italy
[7] Faculty of Science and Technology, University of Twente, PO Box 217, 7500 AE Enschede, The Netherlands
[8] Department of Fusion and Elementary Particle Physics, CIEMAT, Avenida Complutense 22, 28040 Madrid, Spain
[9] Department of Theoretical Electrical Engineering, Technical University of Berlin, Einsteinufer 17, 10587 Berlin, Germany
[10] Physics Department, Milano University, via Celoria 16, 20133 Milano, Italy

Received 27 October 2005, in final form 27 January 2006
Published 15 February 2006
Online at stacks.iop.org/SUST/19/S67

Abstract

The Next European Dipole (NED) Joint Research Activity was launched on 1 January 2004 to promote the development of high-performance Nb_3Sn conductors in collaboration with European industry (aiming at a non-copper critical current density of 1500 A mm^{-2} at 4.2 K and 15 T) and to assess the suitability of Nb_3Sn technology to the next generation of accelerator magnets (aiming at an aperture of 88 mm and a conductor peak field of ∼15 T). It is part of the Coordinated Accelerator Research in Europe (CARE) project, which involves eight collaborators, and is half-funded by the European Union. After briefly recalling the Activity organization, we report the main progress achieved over the last year, which includes: the manufacturing of a double-bath He II cryostat for heat transfer measurements through Nb_3Sn conductor insulation, detailed quench computations for various NED-like magnet configurations, the award of two industrial subcontracts for Nb_3Sn conductor development, the first results of a cross-calibration programme of test facilities for Nb_3Sn wire characterization, detailed investigations of the mechanical properties of heavily cold-drawn Cu/Nb/Sn composite wires, and the preliminary assessment of a new insulation system based on polyimide-sized glass fibre tapes. Last, we briefly review the efforts of an ongoing Working Group on magnet design and optimization.

(Some figures in this article are in colour only in the electronic version)

 © 2006 IOP Publishing Ltd Printed in the UK

1. Introduction

The Next European Dipole (NED) is a Joint Research Activity (JRA) of the Coordinated Accelerator Research in Europe (CARE) project, funded under the auspices of EU-FP6 Research Infrastructures [1]. CARE attempts the integration of high-energy-physics-related accelerator research and development (R&D) in Europe, with a total budget of 35.1 million euros and an EU grant of 15.2 million euros, shared between 22 contractors and ∼100 associated institutes and industrial partners. Besides the NED, CARE includes three network activities (NAs): hadron beams (HHH), electron beams (ELAN) and muon beams (BENE), and three other JRAs: superconducting radio-frequency (SRF), charge production with photo injector (PHIN) and high-intensity proton pulsed injector (HIPPI). Work began on 1 January 2004 and will extend over 5 years.

The initial NED proposal had three main goals [2, 3]:

- to foster a synergy of efforts among European laboratories involved in high-field accelerator magnet R&D,
- to promote the development of high-performance Nb_3Sn wires and cables in collaboration with European industry (aiming at a non-copper critical current density of 1500 A mm^{-2} at 4.2 K and 15 T),
- to get ready for a luminosity upgrade of the Large Hadron Collider (LHC) (foreseen in 2015) [4, 5], and beyond, for LHC energy upgrade or a super LHC [6], by building a large-aperture (88 mm), high-field (15 T conductor peak field) dipole magnet model.

Such a programme would have complemented efforts carried out in the USA within the framework of the US LHC Accelerator Research Program (LARP) [7] or as part of the base programmes at Fermi National Accelerator Laboratory (FNAL) [8] and at Lawrence Berkeley National Laboratory (LBNL) [9]. Unfortunately, the EU allocation was capped to ∼1 million euros (instead of the requested 4 million), which forced a review, and, in the end, the detailed design, manufacture and test of the magnet model was left out of the CARE contract.

At present, the NED Activity is articulated around four Work Packages and one Working Group, which (save for the first one) will be detailed in subsequent sections:

- Management and communication (M&C).
- Thermal studies and quench protection (TSQP).
- Conductor development (CD).
- Insulation development and implementation (IDI).
- Working Group on magnet design and optimization (WGMDO).

In spite of the limited EU funding, the NED is supported by a very active and very enthusiastic collaboration made up of eight partners: CCLRC/RAL (UK), CEA (France; Coordinator), CERN (international), CIEMAT (Spain), INFN-Genova and INFN-Milan (Italy), Twente University (The Netherlands), and Wroclaw University of Technology (Poland). Detailed updates on the work in progress are regularly posted on the NED web site maintained by Twente University [10].

Since the launching of the NED, INFN approved on 30 November 2004 a research project, called CANDIA (Italian acronym standing for CAvi in Niobio-stagno per DIpoli ad Alto campo, or niobium-tin cables for high-field dipoles), involving teams from INFN-Frascati (LNF), INFN-Genova and INFN-Milan (LASA). The main goal of CANDIA is the development of a Nb_3Sn conductor according to NED-like specifications, and a call for tender was issued in the fall of 2005. Of course, close ties will be maintained between CANDIA and the NED.

For reference, table 1 illustrates the position of the NED within the global roadmap of high-field magnet development for large physics instruments, while table 2 presents an inventory of accelerator magnet needs for high-energy physics (HEP) in the mid to long term [5].

2. Thermal studies and quench protection (TSQP) work package

Work Package 2 includes two main tasks:

- Development and operation of a test facility to study and characterize heat transfer to helium through Nb_3Sn conductor insulation and optimization of magnet cooling scheme (involving CEA, CERN and Wroclaw University, under the supervision of CEA).
- Quench protection computation (carried out by INFN-Milan).

2.1. Heat-transfer measurement task

2.1.1. Aim of the study. One of the key issues in the operation of a superconducting particle accelerator is the temperature margin of the dipole and quadrupole magnets the most exposed to beam losses and the ability of the cryogenic system to cope with the deposited energies. In the case of the LHC, the temperature margins of the superconducting magnet coils operated in superfluid helium is mainly determined by the heat transfer coefficient through the polyimide insulation wrapped around the NbTi-based, Rutherford-type cables [11]. Extensive measurements of this coefficient have been carried out at CEA/Saclay in the 1990s on various types of insulation systems and an optimum solution was chosen for the cables of the LHC arc dipole and quadrupole magnets [12]. Furthermore, the geometry of the cooling channels inside the magnet cold masses as well as the diameters of the pipes connecting the various cryogenic elements were dimensioned to ensure a proper extraction of the energy deposited by beam losses.

Wherever NED-like magnets are implemented, they will be subjected to beam losses, and thereby, to energy depositions, which are likely to be higher than those presently foreseen in the LHC. Furthermore, 'wind and react' Nb_3Sn coils call for the use of insulation schemes that are very different from the polyimide wraps applied in LHC magnets (see section 4) and which have never been thoroughly investigated on the thermal point of view. Hence, the issues of temperature margin and magnet cooling must be reassessed to determine what the operational limits of this kind of magnet are.

2.1.2. Task organization and present status. The efforts on assessing the thermal behaviour of NED-like magnets are presently articulated around three sub-tasks:

Table 1. High-field magnet development roadmap for large physics instruments.

Technology	Project/machine	Application	Field	Year
Cu (resistive)	LEP, ESRF Soleil, Diamond	Misc.	up to 2 T	1970s
NbTi, 4.2 K	Tevatron	HEP	4 T	1983
NbTi, 1.9 K	Tore Supra	Fusion	9 T[a]	1988
NbTi, 1.9 K	LHC	HEP	8.33 T	2007
NbTi, 1.9 K	*NEUROSPIN*[b]	*Medical*	11.74 *T*[a]	*2008–2009?*
Nb_3Sn, 4.2 K	ITER/EDA	Fusion	12 T[a]	1995–2000
	ITER			*>2010?*
Nb_3Sn	**CARE/NED**	**HEP**	**14–15 T**	**2004–2008**
	LHC luminosity upgrade			*2015?*
	ILC interaction regions			*mid-2010s?*
	LHC energy doubler			*>2020?*
Nb_3Sn, 1.8 K	*1 GHz NMR*	*Misc.*	23.5 *T*[a]	*2006–2007?*
HTS	*LHC energy tripler*	*MEP*	*24–25 T*	*>2030?*

[a] Conductor peak field.
[b] NEUROSPIN is a full-body, 500 MHz, MRI system under consideration at CEA.

Table 2. Accelerator magnet needs for high-energy physics [5].

Project	Magnet type	Implementation/ quantity	Year	Comment
LHC luminosity upgrade	Large-aperture, high-performance dipole and/or quadrupole magnets	Interaction regions/ a few units	2015	Cost is not an issue
International linear collider (ILC)	LHC-type quadrupole magnets in a solenoidal field or compact quadrupole magnets	Interaction regions/ a few units	mid 2010s	Cost is not an issue
LHC energy upgrade or super LHC	High-performance dipole and quadrupole magnets	Arcs/a large number	*>2020*	Cost is an issue

- Reanalysis of existing cold test data from LHC magnet models relying on optimized NbTi conductor insulation systems.
- Study and characterization of heat transfer coefficient through Nb_3Sn conductor insulation systems.
- Review and modelling of magnet cooling modes to optimize energy extraction.

The LHC magnet test data reanalysis is being carried out at CERN and should be completed by early 2006. Its goal is to verify whether or not the high heat-transfer coefficients measured at CEA on dedicated samples are also observed in actual magnets and to assess the suitability of the CEA sample configuration. It is based on a review of quench data and of AC-loss measurement as a function of ramp rate and will be compared to similar work carried out at FNAL on LHC insertion region quadrupole magnet models [13].

The effort to measure heat transfer coefficients through Nb_3Sn conductor insulation systems makes up the core of this task and will be detailed hereafter. The first part of this effort was devoted to the design and manufacturing of a new double-bath, helium II cryostat.

In parallel, CERN has undertaken a review of cooling modes and has come to the preliminary conclusion that the most efficient one remains pressurized superfluid helium as chosen for the LHC. In addition to more efficient heat removal capabilities, pressurized superfluid helium also offers the side benefit of the critical current enhancement provided by operating the Nb_3Sn conductor at a lower temperature (although not as large as for NbTi, this enhancement is still sizeable). As a result, it is likely that NED-like magnets will have to be operated at 1.9 K. The effort on magnet cooling optimization will be pursued within the framework of an existing collaboration between CERN and Wroclaw University of Technology.

2.1.3. Cryostat design and manufacturing. Measuring heat-transfer coefficient in pressurized superfluid helium environment requires a double-bath cryostat with stringent requirements on temperature control and stabilization. Such a facility existed at CEA/Saclay, but it was decommissioned in the late 1990s because it had become too problematic to operate. Hence, a new cryostat had to be designed and built. CEA developed the conceptual design and wrote detailed specifications that were handed out to Wroclaw University in June 2004. Figure 1 illustrates the proposed conceptual design. Wroclaw University performed a call for tender in the summer of 2004 and selected Kriosystem in Poland to manufacture the cryostat[11]. Work started at Kriosystem in the fall of 2004 and a Production Readiness Review was held at CEA/Saclay on 29 October 2004. The manufacture of the cryostat and of the enclosed heat exchanger was completed by early spring 2005 and preliminary reception tests were carried out on Kriosystem's premises the third week of April. After a few modifications and improvements, a second round of reception tests was carried out in Wroclaw on 6–8 July 2005. These tests included thermal and leak tests in liquid helium environment at 4.2 K and were deemed successful. Since then, the cryostat

[11] Kriosystem, 18 Muchoborska Street, 54-424 Wroclaw, Poland.

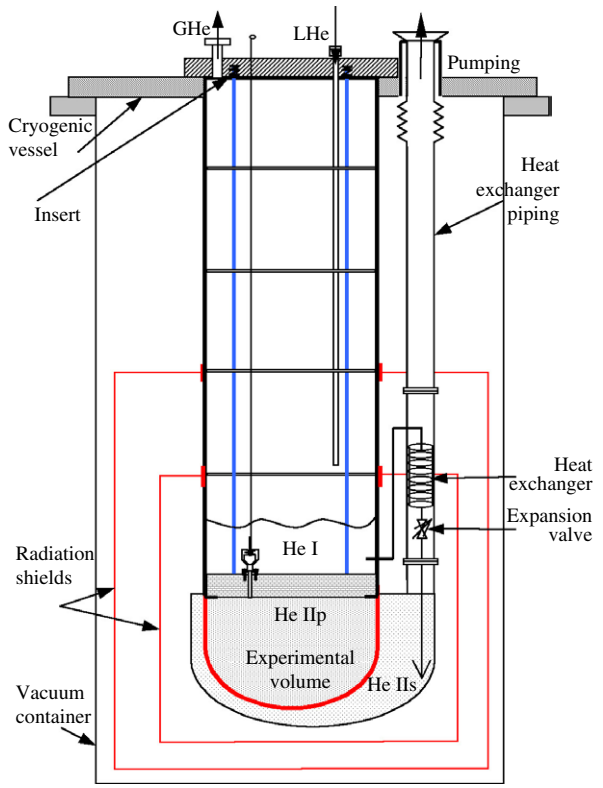

Figure 1. Conceptual design of double-bath cryostat for heat-transfer measurements developed by CEA/Saclay. (Reprinted by permission © 2005 IEEE) [3].

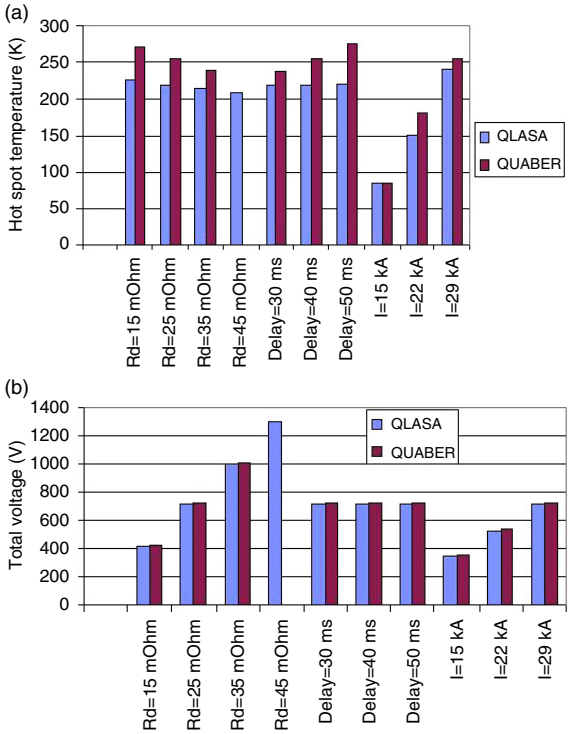

Figure 3. Comparison of quench computations carried out at INFN-Milan with QLASA and QUABER codes on 10 m long, 88 mm aperture, ($\cos\theta$, layer) NED Reference Design V1: (a) hot-spot temperature (top) and (b) total coil voltage (bottom).

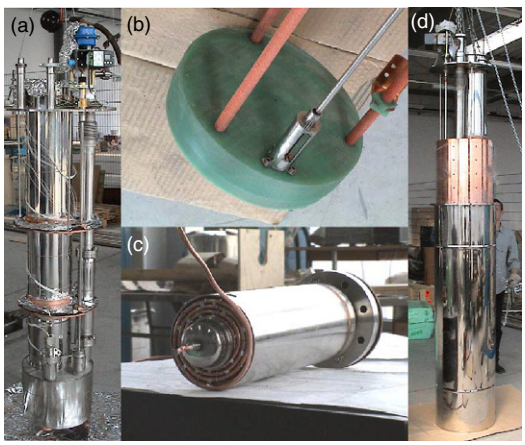

Figure 2. Various pictures of the NED cryostat and of its critical components manufactured by Kriosystem in Poland, under the supervision of Wroclaw University of Technology: (a) inner assembly with instrumentation (left), (b) lambda plate (middle top), (c) heat exchanger (middle bottom) and (d) final assembly with thermal shields (right).

has been transported by road to CEA/Saclay, where it arrived on 20 September 2005. It is now being prepared for tests in superfluid helium and commissioning. The first measurements are expected to take place in early 2006. Figure 2 presents various pictures of the cryostat and of its critical components.

2.2. *Quench computation task*

The magnetic energy stored in NED-like magnets is considerably higher than for NbTi dipole and quadrupole magnets of similar aperture, thereby raising the issue of quench protection. Hence, careful and thorough modelling of the quench behaviour is needed to ensure that such magnets can be operated safely. In the case of the NED, the aim is to limit hot-spot temperature to 300 K and coil voltages to 800 V.

After completing a literature survey of relevant material properties (and having verified that the variability in available data did not dramatically affect salient computation results [3]), INFN-Milan carried out detailed quench studies on the 88 mm aperture, $\cos\theta$, layer design chosen as Reference Design V1 (see section 3.1 and figure 4(a)). The computations have investigated the influence of various parameters such as:

- magnet length (1, 5 and 10 m),
- operating current (15, 22 and 29 kA),
- value of external dump resistor (15, 25, 35 and 45 mΩ),
- quench detection delay (30, 40 and 50 ms),
- quench protection heater length.

They have been carried out using two independent computer codes:

- QLASA, originally developed at INFN-Milan for solenoids [14], and subsequently adapted to accelerator magnet coil configuration by means of suitable geometric approximations,
- QUABER, a collection of scripts written in MAST and run with the commercial SABER® software package [15] that was developed at CERN to study LHC magnet protection [16].

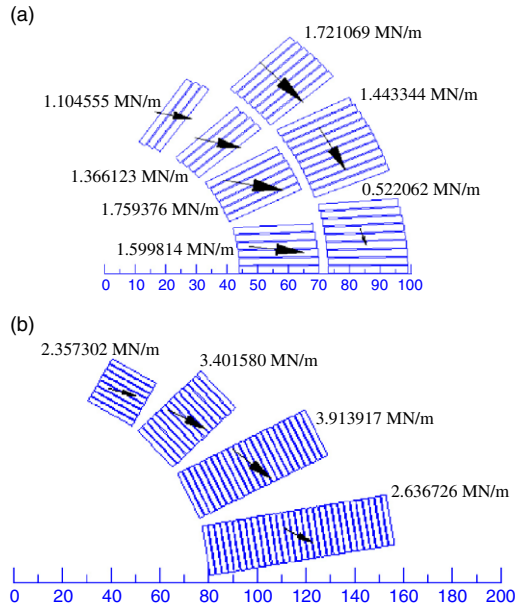

Figure 4. Conductor and Lorentz force distribution in top right quadrant of two NED preliminary designs developed by CERN: (a) 88 mm aperture, $\cos\theta$, layer design (chosen as Reference Design V1; top) and (b) 160 mm aperture, $\cos\theta$, slot design (bottom) (reprinted by permission © 2005 IEEE) [3].

Table 3. Selected NED wire parameters [3].

Parameter	Value
Strand diameter	1.250 mm
Effective filament diameter	$<50\ \mu$m
Cu-to-non-Cu volume ratio	1.25 ± 0.10
Filament twist pitch	30 mm
Non-Cu J_C at 15 T and 4.2 K	1500 A mm^{-2}
Minimum critical current	1636 A at 12 T
at 4.2 K	818 A at 15 T
RRR (after full reaction)	>200
N-value at 15 T and 4.2 K	>30

Table 4. Salient parameters of Rutherford-type cable for 88 mm aperture, $\cos\theta$, layer design chosen as the NED Reference Design V1 [3].

Parameter	Value
Cable width	26 mm
Cable mid-thickness at 50 MPa	2.275 mm
Keystone angle	0.22°
Number of strands	40
Critical current at 4.2 K, with	29440 A at 15 T
field normal to broad face	58880 A at 12 T
Minimum critical current	736 A at 15 T
at 4.2 K of extracted strand	1472 A at 12 T
RRR after reaction	$\geqslant 120$
Minimum cable unit length	145 m

The results of the INFN-Milan study are detailed in [17] and are illustrated in figures 3(a) and (b), which summarize hot-spot temperature and total coil voltage plots obtained for the 10 m long case. The QLASA and QUABER computations concur to show that, within the investigated parameter space, the hot-spot temperature always remains below 300 K while the coil voltages can be limited to 800 V by an adequate choice of external dump resistor (which should be no larger than 25 mΩ). The 1 m long magnet does not require active protection, while the 5 m long and the 10 m long versions do require quench heaters, covering at least 80% of the length of the coil outer layer and being able of quenching it within 40–50 ms of their firing. These very encouraging results confirm the suitability of the wire and cable parameters chosen early on in the programme and prove that quench protection should be an issue for the NED.

To wrap up its effort, INFN-Milan has now undertaken quench computations on the more challenging 160 mm aperture, $\cos\theta$, slot design shown in figure 4(b).

3. Conductor development (CD) work package

Work Package 3 makes up the core of the NED Activity and absorbs about 70% of the EU funding allocation. It includes three main tasks:

- conductor development (under CERN supervision),
- conductor characterization (involving CEA, CERN, INFN-Genova, INFN-Milan and Twente University, under the supervision of Twente University),
- finite element (FE) wire model to simulate cabling effects (involving CERN and INFN-Genova, under the supervision of INFN-Genova).

Note that the FE wire model task is an extension of scope with respect to the CARE contract.

3.1. Conductor development

3.1.1. Preliminary designs and conductor parameters. CERN launched its NED efforts in 2003 by carrying out preliminary magnetic design studies for high-field and large-bore dipole magnets that were aimed at deriving meaningful Nb_3Sn wire and cable specifications. Two different magnetic configurations were investigated using the ROXIE software package [18]: the conventional $\cos\theta$, layer design and a more innovative $\cos\theta$, slot design, first proposed by Pérot at CEA/Saclay in the early 1980s [19]. Three apertures were considered: 88, 130 and 160 mm. As an illustration, figure 4(a) shows the 88 mm aperture layer design, while figure 4(b) shows the 160 mm aperture slot design.

The preliminary investigations led to the definition of a common wire that can be made into different Rutherford-type cables suitable to the various magnetic designs under consideration. Salient parameters of this wire are summarized in table 3. Furthermore, the 88 mm aperture, $\cos\theta$, layer design of figure 4(a) has been chosen as Reference Design V1 for the NED. Thanks to the cable parameters summarized in table 4 (which assume a 10% critical current degradation with respect to virgin wires), it produces a central field of 14.4 T at 28.7 kA, with an inductance of 4.4 mH m^{-1} and a stored magnetic energy of 1.8 MJ m^{-1} (the conductor peak field is in excess of 15 T). These wire and cable parameters form the basis of the NED conductor specifications. Let us stress that the reliance on a large conductor and a large transport current is a deliberate choice that differentiates the NED from other programmes and is one of the reasons why the quench protection issue is not so critical (see section 2.2).

3.1.2. Cable contracts. Following the write up of comprehensive wire and cable specifications and of a detailed

technical questionnaire, CERN issued a call for tender in June 2004 and, in November 2004, selected Alstom/MSA, in France[12], and ShapeMetal Innovation (SMI), in the Netherlands[13], to be the main wire and cable contractors. After discussion with CERN, the two companies have established development plans made up of two R&D steps (referred to as STEP1 and STEP2) followed by final production. For Alstom/MSA, which promotes the 'enhanced internal tin (EIT)' process, STEP1 is devoted to a Taguchi-type plan to study the influence of salient parameters on workability and performances, while STEP2 will be devoted to a tuning of critical current density. For SMI, which promotes the 'powder in tube (PIT)' process, STEP1 is devoted to iterations on an existing, 1 mm diameter, wire design, which has reached a non-copper critical current density of 2500 A mm^{-2} at 4.2 K and 12 T, while STEP2 will be devoted to a scale-up to larger-size billets. The results of STEP1 are expected in the fall of 2005, and those of STEP2 in the summer of 2006, while the final cables should be delivered in December 2006.

3.2. *Conductor characterization*

3.2.1. Working group on conductor characterization (WGCC). The NED conductors will be characterized by performing detailed RRR, critical current and magnetization measurements. The critical current measurements are particularly challenging given the unprecedented performances that are expected, e.g.: ∼1600 A at 4.2 K and 12 T on a 1.25 mm diameter wire, to be compared to the ∼200 A presently achieved on 0.81 mm diameter ITER wires. A working group on conductor characterization (WGCC), made up of representatives from CEA, CERN, INFN-Genova and INFN-Milan and chaired by Twente University, was set up in the spring of 2004 to oversee these measurements. The working group is charged with the definition and development of standardized procedures to measure the properties of virgin, deformed and extracted strands and has the responsibility for certification of the measured data.

3.2.2. Critical current measurements. Inspired by the VAMAS and ITER/EDA programmes, [20, 21], the working group has initiated a cross-calibration of the critical-current measurement facilities at CEA, INFN-Milan and Twente University. The cross-calibration programme has proven to be more difficult than anticipated. Three rounds of *virgin* test wires have been circulated among the collaborators, including a reference, LHC-type, NbTi wire provided by CERN and two Nb_3Sn wires provided by Twente University: an old PIT wire of large diameter (1.26 mm) produced by the Energy research Center of the Netherlands (ECN), but whose critical current turned out to be somewhat heterogeneous along its length, and a more recent SMI PIT wire, of smaller diameter (1 mm), but of large and homogenous critical current (in excess of 1000 A at 4.2 K and 12 T). The tests on virgin wires were complemented by tests on samples of an old, 0.83 mm diameter, internal-tin Europa Metalli wire, extracted by INFN-Milan from a Rutherford-type cable, and by tests on samples of the ECN PIT wire rolled down by CERN so as to flatten with a diameter reduction of 0.35 mm along the flattening direction. The tests on *extracted* and *deformed* wires were intended as preparatory investigations of cabling degradation.

The cross-calibration measurements have pointed out a number of problems and discrepancies in sample preparation and instrumentation as well as in measurement procedures, which have been identified, assessed and have been or are being corrected. Two out of the three laboratories involved have now achieved a good convergence on virgin wires (their results for the SMI PIT wire agree within 2%); the dispersion is somewhat larger for the deformed wires (5–7% on the rolled ECN PIT wire), but, as already mentioned, this may be due to heterogeneities in the wire itself. The third laboratory is still in the process of upgrading its equipment, but should be ready on time when the first STEP1 wires will become available from the manufacturers. Comprehensive descriptions of the NED cross-calibration programme and of the sample mounting and measurement procedures that have been agreed upon are given in [22].

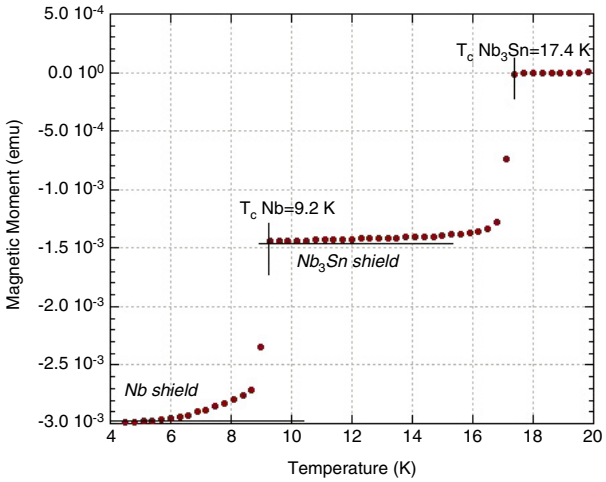

Figure 5. Magnetization measurements as a function of temperature in a 10 mT parallel field performed on a reacted ECN PIT wire sample with a SQUID magnetometer (courtesy of C Ferdeghini, INFM-Genova).

3.2.3. Magnetization measurements. In parallel to the efforts on critical current measurement, INFN-Genova has carried out a series of magnetization measurements with different types of apparatus to evaluate their respective pertinence:

- a SQUID magnetometer at INFM/Genova (courtesy of C Ferdeghini),
- a vibrating sample magnetometer (VSM) at INFN-Frascati (courtesy of U Gambardella),
- an AC-susceptibility magnetometer available in house.

These measurements were carried out either as a function of field, in view of assessing effective filament diameter and the amplitude of flux jumps, or as a function of temperature, to study the nature and size of the various superconducting phases present in the wire.

As an illustration, figure 5 presents magnetization measurements performed as a function of temperature (in

[12] Alstom Magnets and Superconductors (MSA), 3 Avenue des trois chênes, 90018 Belfort Cedex, France.
[13] ShapeMetal Innovation BV, Het Lentfert 31, 7547 SN Enschede, The Netherlands.

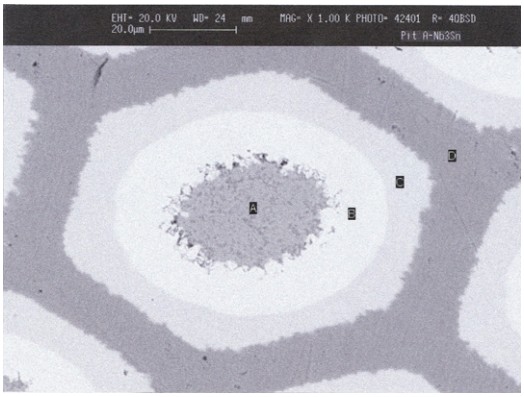

Figure 6. Backscatter electron micrograph of a reacted tube in an ECN PIT wire (courtesy of C Ferdeghini, INFM-Genova). From the inner to the outer: (A) powder residue (dark grey), (B) layer of reacted Nb_3Sn (white), (C) sheath of unreacted Nb (light grey) and (D) pure copper matrix (dark grey).

a 10 mT parallel field) with a SQUID magnetometer on a sample of the 1.26 mm diameter ECN PIT wire mentioned above. The plot clearly shows two transitions: one for a temperature of ∼17.4 K, corresponding to Nb_3Sn, and one around 9.2 K, corresponding to pure Nb. The origin of these two transitions can be readily understood when considering the wire structure: it is drawn down from a billet made up from thick-walled niobium tubes, arranged in a pure copper matrix and stuffed with a mixture of $NbSn_2$, Cu and Sn powders. During heat treatment, the powder mixture reacts with the Nb tubes and precipitate Nb_3Sn layers, which grow from the inner to the outer radii of the tubes. The heat treatment is usually optimized so as to react about two-thirds of the tube walls, thereby leaving a sheath of unreacted niobium at the tube periphery, as illustrated on the backscatter electron micrograph of a reacted tube displayed in figure 6. As a result, when cooling down the ECN PIT wire to cryogenic temperatures in a small background magnetic field, a first transition occurs when the Nb_3Sn layers on the inner part of the tubes become superconducting, and a second transition follows when the unreacted Nb sheaths on the outer part of the tubes, in turn, become superconducting. Furthermore, the amplitudes of the magnetizations measured in these two stages enable one to determine the magnetically shielded volumes which are associated and, thereby, the outer diameters of the reacted Nb_3Sn layers and of the unreacted Nb tubes. In our example, we get 44 μm for the Nb_3Sn layers and 65 μm for the Nb tubes. These values are in good agreement with the physical values that can be estimated from the SEM image of figure 6. A detailed summary of the preliminary investigations carried out by INFN-Genova can be found in [23], which also exhibits experimental evidences that part of the large flux jumps observed on this wire may originate in the unreacted Nb phase.

3.3. FE wire model

The NED wires will undergo cabling operations to form Rutherford-type cables. During such operation, the wires are inelastically and permanently deformed, which can cause buckling and/or breakage of filaments and/or internal barriers and lead to irreversible degradations of wire properties. Hence, it is crucial when developing new wires to assess their sensitivity to cabling and to optimize their design to limit the risks of cabling degradation.

In addition to direct tests on deformed wires, as presently evaluated by the working group on conductor characterization (see section 3.2), an effort has been launched by INFN-Genova to build a finite element (FE) mechanical model of unreacted wires aimed at simulating cabling deformations. The model, developed in ANSYS®,[14] was first applied to an old, 19 subelement, internal tin wire manufactured by Alstom/MSA for CEA/Saclay [24]. However, it quickly appeared that, to be accurate, one needed a detailed knowledge of the stress–strain curves of the materials making up the wire in the cold work state where they are at the time of cabling. For the FE computations, it was assumed that the stress–strain curves can be described by bilinear functions, which reduced the number of parameters to be determined for each material to only four: Young's modulus, yield strength, ultimate tensile strength and elongation at breakdown.

Determining suitable values of material properties was somewhat arduous. At first, CERN carried out a literature survey but found some inconsistencies and decided to launch several types of measurements on unannealed and unreacted samples of the 19-subelement Alstom/MSA wire. These measurements included: micro-hardness measurements performed at CERN, nano-hardness measurements subcontracted to Ecole d'Ingénieurs de l'Arc Jurassien (EIAJ, located in Le Locle, Switzerland), tensile tests on wires performed at CERN, tensile tests on wires and single Nb-Ta filaments extracted from the wires subcontracted to BundesAnstalt für Materialforschung (BAM, located in Berlin, Germany), and RRR measurements performed at CERN (to cross-check the rate of cold work of the high-purity copper in the wire). As an illustration, figure 7(a) shows an example of a matrix of imprints left by micro-hardness measurements performed at CERN on a wire cross-cut while figure 7(b) shows an example of a matrix of imprints left by nano-hardness measurements performed at EIAJ on a longitudinal cut of the same wire. The data from the various tests have now been analysed, cross-checked and compared with available literature data and are summarized in table 5, which presents a best guess on the material properties of the unannealed and unreacted, 19-subelement, Alstom/MSA wire. These values are ready for implementation in the FE model.

The present plan calls for INFN-Genova to study the behaviour of two types of internal tin wire developed by Alstom/MSA: the old, 19-subelement design and the new NED designs. In parallel, CERN will launch a new effort to assess the mechanical properties of unreacted PIT wires.

4. Insulation development and implementation (IDI) work package

4.1. Aim of the study

At present, most accelerator magnet coil designs call for small bending radii in the coil heads, which cannot be forced upon

[14] ANSYS®, Inc., Southpointe, 275 Technology Drive, Canonsburg, PA 15317, USA http://www.ansys.com/

Table 5. Best guess on material properties of unannealed and unreacted, 19-subelement, internal tin wire developed by Alstom/MSA for CEA.

Material	Young's modulus (GPa)	Yield strength @0.2% (MPa)	Ultimate tensile strength (MPa)	Elongation at breakdown (%)
Cu	112	350	385	1.5
Sn	44.3	14.5	14.5	65
Nb (barrier)	103	880	915	3
NbTa (filament)	117	915	980	3
Ta (barrier)	186	1110	1165	3

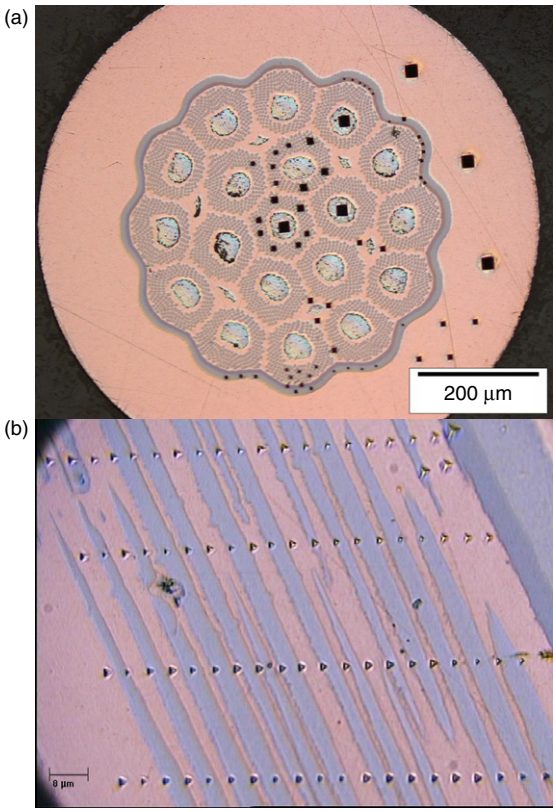

Figure 7. Examples of matrices of imprints left by hardness measurements on cuts of an old, unannealed and unreacted, 19-subelement, internal-tin wire produced by Alstom/MSA for CEA: (a) micro-hardness measurements performed at CERN on a cross cut (top) and (b) nano-hardness measurement performed at EIAJ on a longitudinal cut (bottom).

a reacted Nb_3Sn cable without deleterious degradations. As a result, Nb_3Sn accelerator magnet coils are produced by the so-called 'wind and react' process, where coil winding is performed with unreacted conductors and a heat treatment is applied to the whole coil upon winding completion to precipitate Nb_3Sn [25]. This heat treatment is carried out in a vacuum or in a flow of inert gas such as argon to prevent oxidation of the OFHC copper stabilizing the conductors. The heat treatment parameters depend on wire design (e.g., internal tin or powder in tube), but the cycle always includes a high-temperature plateau between 650 and 700 °C for a few tens to a few hundreds of hours.

A direct consequence of the application of a heat treatment on the whole coil is that the conductor insulation must be able to sustain the high-temperature plateau. This precludes the polyimide tapes commonly used in NbTi accelerator magnets. The most conventional insulation system for 'wind and react' Nb_3Sn coils is to rely on glass or ceramic fibre tapes or braids, which are wrapped or sleeved or woven around the unreacted conductors prior to winding, and, subsequently, upon heat treatment completion, to transfer the reacted coil from its heat treatment retort to a vacuum-impregnation mould, and to vacuum-impregnate it with epoxy resin [25].

The reliance on thin fibre tapes, which, as explained in section 4.3, must be de-sized from all organic components to prevent the formation of carbon residues during the high-temperature cycle, and the inherent difficulties of performing a vacuum impregnation on fragile coils complicate notably the manufacturing process, raise costs and failure risks and limit its potential for industrial applications. As an alternative, CEA/Saclay has been working on an innovative insulation scheme, which relies on a glass fibre tape, pre-impregnated with an inorganic solution of precursors. The pre-impregnation restores the tape mechanical strength while maintaining a suitable flexibility, which enables cable wrapping and conductor winding with little degradation. Furthermore, during heat treatment, the precursors of the pre-impregnation undergo a ceramic-like phase transition, which bonds the turns together and confers a rigid shape to the coil, thereby eliminating the need for a subsequent vacuum-impregnation. If successful, the innovative insulation system would provide an elegant solution to the insulation problem of 'wind and react' coils, that both simplifies the manufacturing process and reduces the risks associated with the handling of reacted Nb_3Sn cables.

The aim of Work Package 4 is to pursue the parallel development of the two types of insulation. Consequently, it is articulated around two main tasks:

- conventional insulation (carried out by CCLRC/RAL),
- innovative insulation (carried out by CEA).

4.2. Engineering specification

Before launching their efforts, CCLRC/RAL and CEA wrote an engineering specification for the conductor insulation of NED-like, 'wind and react,' Nb_3Sn magnets (issued in July 2004) and agreed on a coordinated test programme for both conventional and innovative insulations (issued in October 2004). Table 6 summarizes the most salient mechanical, thermal, and electrical requirements that make up the specification as well as a first guess on the radiation doses that should be sustained.

Table 6. The NED conductor insulation specifications [3].

General	Design
Insulation thickness per cable	0.4 mm
Winding compatibility: Capable of being applied to the cable and formed into a dipole winding by a semi-automatic winding system	Minimal fraying or abrasion during winding
Conductor bend radius minimum	20 mm
Compatible with Nb_3Sn heat treatment cycle	Minimal degradation of basic components
Thermal cycles to low temperature: 300–4.2 K	10
Running cycles: ramp to maximum compressive stress	100
For conventional organic insulation scheme and innovative scheme if applicable: ability to be impregnated with a liquid of viscosity 200 mPa s	200 mPa s

Mechanical[a]	Design
Applied conductor winding load	500 N
Compression during heat treatment	20 MPa
Coil reshaping after heat treatment and before impregnation	20 MPa
Compressive stress after completion of coil fabrication—at 300 K and 4 K.	200 MPa
Shear: short-beam shear strength at 4 K	50 MPa
Tension: transverse tensile strength of insulation laminate at 4 K	25 MPa
Fracture, need to know properties at 300 and 4 K, specification to be determined	TBD

Thermal	Design
Transverse thermal contraction (integrated between 300 and 4 K)	0.003–0.004
Thermal conductivity at 4.2 K	50 mW m^{-1} K^{-1}

Electrical	Design	Failure
Breakdown voltage inter-turn tested in helium at 300 K	1000 V 2500 V mm^{-1}	2000 V 5000 V mm^{-1}

Radiation	
The failure properties above must be achieved following doses expected during 10 years' running.	
Dose	50–600 MGy
Fluence >0.1 MeV	2.5–30 × 10^{16} cm^{-2}

[a] Design stresses are before irradiation.

4.3. Conventional insulation

CCLRC/RAL has developed a standardized laminate production system and relies on three tests to screen candidate materials for conventional insulation:

- inter-laminar fracture test,
- short-beam shear test,
- electrical breakdown test.

Figure 8 shows an example of a double cantilever beam (DCB) sample used for fracture tests. The standard laminates leave sufficient material for future radiation testing. Details on this ongoing programme can be found in [26] while table 7 summarizes the most salient results.

To gain experience and validate the inter-laminar fracture tests, three know systems of epoxy resin have been investigated:

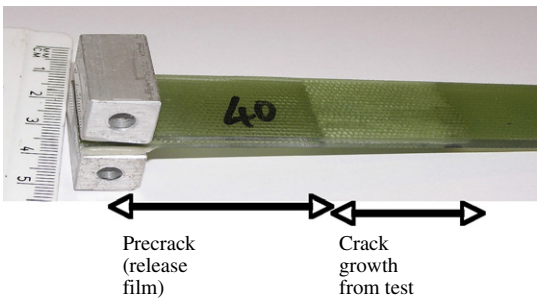

Figure 8. Example of double cantilever beam (DCB) fracture test carried out at CCLRC/RAL.

- a brittle system made up of DGEBA resin with an acid anhydride hardener (HY918, Ciba),

Table 7. Salient results from conventional insulation screening tests at CCLRC/RAL [26].

Fabric	Sizing	Treatment	Resin/ hardener	Work of fracture at 300 K (kJ m^{-2})	Short beam shear strength at 77 K (MPa)	Breakdown voltage (kV mm^{-1})
E glass	Regular	As received	DGEBA/ anhydride acid	0.45		
		As received	DGEBF/ aromatic amine	0.8		
		As received	DGEBA/ aliphatic amine	1		
S glass	Regular	As received	DGEBF/ DETDA	0.49	94	>30
		Heat treated[a] (w/o de-sizing)	DGEBF/ DETDA			2.5
		De-sized and heat treated[a]	DGEBF/ DETDA	Not meaningful[b]	69	
S glass	Polyimide	As received	DGEBF/ DETDA	0.7	89	
		Heat treated[a] (w/o de-sizing)	DGEBF/ DETDA	0.67	98	>30

[a] At 660 °C for 60 h in a vacuum.
[b] Sample failed through the glass layer and not in an inter-laminar fashion.

- a tough system, made up of DGEBA resin with an aliphatic amine hardener (Jeffamine D-400),
- an intermediary system, made up of DGEBF resin, a PPGDGE flexibilizer and an aromatic amine hardener (HY5200, Ciba).

All samples were prepared using as-received E-glass tapes with commercial sizing, and the tests were performed at room temperature and at 77 K. As expected, the brittle system yields the lowest work of fracture (∼0.45 kJ m^{-2} at room temperature), the toughest system yields the highest one (∼1 kJ m^{-2} at room temperature), while the intermediary system is in between (∼0.8 kJ m^{-2} at room temperature). The results are in the same order, but 20 to 40% higher, at 77 K.

CCLRC/RAL has also started to investigate the issue of sizing. As already mentioned, the filaments of commercially available glass fibre tapes are usually coated with a mixture of organic materials, referred to as *sizing*. There are all kinds of sizings, with different functions (such as lubrication during high-speed weaving or enhancement of wetting and chemical-coupling between fibre and matrix during resin impregnation). However, most sizings are not intended for high-temperature use, and, if left in place during the Nb_3Sn reaction cycle, are likely to result in undesirable carbon residues [25]. In practice, the sizing is removed from the tapes by carbonization in air at temperatures in the 350–450 °C range prior to conductor wrapping and winding. The problem is that removing the sizing renders the tape fragile and easy to tear off by friction, which further complicates the already challenging 'wind and react' coil manufacturing process.

To solve this problem, CCLRC/RAL has identified an improved, polyimide, sizing material, produced by Hydrosize, NC, USA[15], which may be able to sustain the Nb_3Sn reaction cycle without serious degradation. The sizing is currently applied to various types of glass and quartz fibre fabrics commercialized by JPS Glass, SC, USA[16]. To assess its suitability to NED-like applications, CCLRC/RAL has undertaken a comparative test on standard laminates made up of conventional S-glass tapes (as received, de-sized and heat treated for 60 h at 660 °C in a vacuum after de-sizing) and of polyimide-sized, S-glass and quartz fabrics provided by JPS (as received and heat-treated for 60 h at 660 °C in a vacuum without de-sizing). The laminates were vacuum-impregnated with a system made up of DGBEF resin (DER354P, Dow) and a DETDA hardener (HY5200, Vantico). (This system was chosen because it is both relatively radiation stable and has a low viscosity, and, thereby, seems the best suited to the NED application). The work of fracture measured on the conventional, as-received, S-glass sample is 0.49 kJ m^{-2} at room temperature, which puts the resin system into the brittle category (not unexpected given the nature of the hardener that was chosen). No meaningful work of fracture could be measured on the conventional, de-sized, heat-treated, S-glass sample. Indeed, the sample failed through the glass layer and not in an inter-laminar fashion, thereby indicating that the glass was adversely affected by heat treatment. The results on the polyimide-sized, S-glass samples are very promising: the work of fracture on the sample made up of as-received fabric is 0.7 kJ m^{-2} at room temperature and stays at 0.67 kJ m^{-2} on the sample made up of heat-treated fabric. The short-beam shear strengths measured at 77 K are above ∼90 MPa for all samples, save for the conventional, de-sized, heat-treated, S-glass sample, where it falls to 69 MPa. Finally, electrical breakdown tests were carried out on conventional, heat-treated, de-sized and not de-sized S-glass samples and on heat-treated, polyimide-sized S-glass samples. The voltage measured on the conventional, de-sized sample and on the polyimide-sized sample are both in excess of 30 kV mm^{-1}, while the one measured on the sample made up of conventional S glass, heat-treated without de-sizing, is degraded to 2.5 kV mm^{-1}.

[15] Hydrosize, 3209 Gresham Lake Road, Suite 109, Raleigh, NC 27615, USA info@hydrosize.com

[16] JPS Composites, Greenville, SC 29607, USA.

Table 8. Comparison of various $\cos\theta$, layer dipole magnet designs with respectto horizontal and vertical Lorentz force resultants computed over a coil quadrant.

Magnet	Technology	Aperture (mm)	Maximum central field (T)	Stored energy (kJ m^{-1})	ΣF_x[c] (MN m^{-1})	ΣF_y[c] (MN m^{-1})
Tevatron	NbTi	76.2	4.4	64	0.5	0.3
HERA	NbTi	75	4.7	83	0.6	0.3
SSC	NbTi	50	6.7	110	0.9	0.4
LHC[a]	NbTi	56	8.3	253[b]	1.6	0.8
MFISC[a] [29]	NbTi	56	10	380[b]	2.1	1.0
MFRESCA [30]	NbTi	87.8	10.15	694	3.4	2.5
MSUT [31]	Nb_3Sn	50	11.5	391	3.25	1.6
D20 [32]	Nb_3Sn	50	13	802	5.6	2.0
NED	Nb_3Sn	88	14.4	1804	7.9	3.9

[a] Twin-aperture design.
[b] Per aperture.
[c] Resultant over a coil quadrant.

At the light of these first results, the S-glass, polyimide-sized fabric provided by JPS appears to satisfied most of the NED mechanical and electrical specifications. The next question that CCLRC/RAL is trying to answer is whether or not the polyimide sizing can be applied to S-glass tapes of the desired thickness (typically ∼0.1 mm).

4.4. Innovative insulation

The feasibility of the innovative insulation scheme has been demonstrated within the framework of an internally funded Nb_3Sn R&D programme at CEA/Saclay. The solution of precursors and its application to the fibre glass tape have been optimized to enable proper pre-impregnation and conductor wrapping [27]. Furthermore, it has been verified that, when subjecting a stack of insulated cables to a temperature cycle representative of the Nb_3Sn heat treatment, the cables bonded together and that the chemical reaction that takes place does not degrade the transport-current properties of Nb_3Sn wires [28]. The next step of the programme is to better characterize and improve the mechanical properties after heat treatment and to reduce the thickness of the pre-impregnated tape. However, the work on innovative insulation has been put on hold at CEA due to a lack of human resources. It is expected to restart in January 2006.

5. Magnet design and optimization (MDO) working group

5.1. Working group charges and roadmap

Although the 88 mm aperture, 15 T (conductor peak field) dipole magnet model, which was included in the initial NED proposal, has been dropped from the final CARE contract, CCLRC/RAL, CEA and CERN have decided to join forces to create an informal Working Group on magnet design and optimization (WGMDO), coordinated by CIEMAT. This working group is an extension of scope with respect to the CARE contract and is mainly supported by additional resources.

Up to now, all superconducting accelerator magnets implemented in operating machines rely on conventional $\cos\theta$ or $\cos 2\theta$, layer designs. The $\cos\theta$, layer design is very effective in terms of field quality (and field quality tuning), peak-to-central-field ratio, and superconductor volume. However, and as illustrated in figure 4(a), it presents one potential disadvantage: the Lorentz forces tend accumulate in the azimuthal direction and can result in high transverse pressures over the midplane conductors. This transverse pressure must be limited to a reasonable value to prevent critical current degradation. Of course, the larger the magnet aperture and the central field, the larger the Lorentz forces. Table 8 summarizes values of horizontal and vertical Lorentz force resultants (computed over a coil quadrant) for a series of $\cos\theta$, layer dipole magnet designs developed over the years. It appears that the Lorentz forces expected in the NED Reference Design V1 are about five times higher than in LHC arc dipole magnets, thereby requiring careful stress management. Consequently, the Working Group has been charged with addressing the following questions.

- How far can we push the conventional, $\cos\theta$, layer design in the aperture versus central field parameter space (especially, when relying on strain-sensitive conductors)?
- What are the most efficient alternatives in terms of performances, manufacturability and costs?

First, the Working Group agreed on a common set of high-field dipole magnet design parameters (see table 9) and on a common set of material properties, such as iron yoke B–H curve (see figure 9) and Young's moduli and integrated thermal expansion coefficients (see table 10). Then, it selected a number of magnetic configurations to be studied and compared, which include:

- the conventional, $\cos\theta$, layer design,
- Pérot's $\cos\theta$, slot design [19],
- a so-called *ellipse-type* design proposed by CEA,
- a so called *motor-type* design proposed by CIEMAT [3],
- the twin-aperture, common-coil design, first proposed by Danby at Brookhaven National Laboratory (BNL) in 1983 [33] and subsequently resuscitated by Gupta in 1996 [34],
- The tilted-solenoid or double-helix design first proposed by Meyer in 1970 [35].

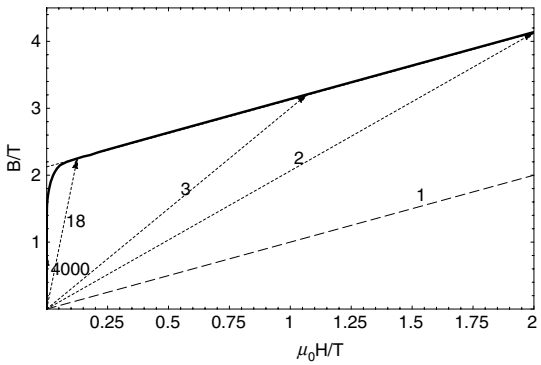

Figure 9. Iron yoke B–H curve used by NED/WGMDO partners for electromagnetic computations.

Table 9. Salient high-field dipole magnet design parameters selected by NED/WGMDO.

Parameter	Value	Units
Peak field on conductor	15	T
Aperture	88-130-160	mm
Reference radius	29-43-53	mm
Superconductor J_C	3000	A mm^{-2} @ 4.2 K and 12 T
	1500	A mm^{-2} @ 4.2 K and 15 T
Cu-to-non-Cu ratio	1.25	
Operating margin	10	%
Filling factor of cable	87	%
Insulation thickness	0.2	mm per conductor face
Cabling degradation	10	%
X-section multipoles	A few 10^{-4}	@ reference radius
Overall coil length	1.3	m
Peak stress	150	MPa
Max. coil deformation	<0.05	mm (due to Lorentz forces)
Peak temperature	300	K (quench)
Peak voltage to ground	1000	V (quench)
Peak inter-turn voltage	100	V (quench)

The comparison will be carried out in three steps: (1) comparison of 2D electromagnetic designs, (2) comparison of 2D mechanical designs and (3) comparison of 3D designs. Each partner has chosen one or two configurations and has started to work on 2D electromagnetic and mechanical designs, but the analyses have not yet achieved a sufficient level of maturity to enable a full-blown comparison.

Before describing the ongoing work, let us introduce customary notations. Let (O, x, y, z) designate a rectangular coordinate system. For the 2D electromagnetic optimizations, the current distributions are assumed to be uniform in z and the magnetic flux density has only two components, B_x and B_y, which are also uniform in z. Then, in the magnet aperture, the magnetic flux density can be expanded into a power series of the form

$$B_y + \mathrm{i}B_x = B_{\mathrm{ref}} 10^{-4} \sum_{n=1}^{+\infty} (b_n + \mathrm{i}a_n) \left(\frac{x + \mathrm{i}y}{R_{\mathrm{ref}}} \right)^{n-1} \quad (1)$$

where B_{ref} is the main dipole field, R_{ref} is the reference radius, and b_n and a_n are the normal and skew $2n$-pole coefficients expressed in so-called *units*.

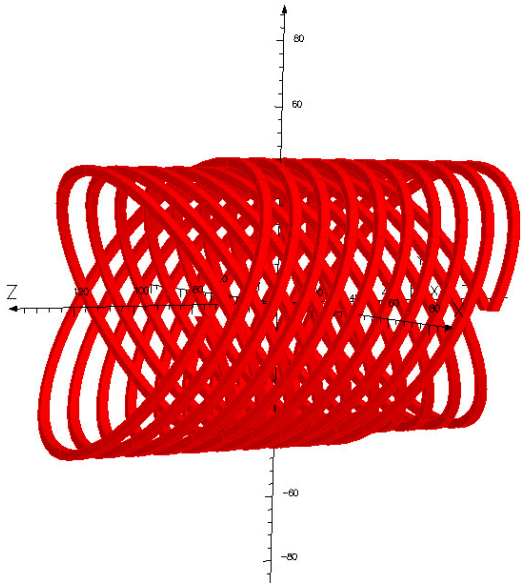

Figure 10. Tilted-solenoid or double-helix configuration under investigation by CCLRC/RAL.

5.2. CCLRC/RAL contribution

CCLRC/RAL has chosen to investigate the Reference Design V1, $\cos\theta$, layer design and to assess the feasibility of a double-helix magnetic configuration. The $\cos\theta$ optimization was carried out using software supplied by the commercial company Vector Fields (VF)[17], which has close links with the RAL magnet group. At first, the software was used to construct a 2D parameterized FE model, which includes the option of modelling the nonlinear effects of iron and a non-uniform current density in the conductor winding (as generated by the slightly-keystoned, NED Rutherford-type cable). A number of test cases were run to check the optimizer provided by Vector Fields and to look at the effects of changing the objective functions. The output from the full model has now been compared with ROXIE (see section 5.4) and it gives the same results for the same geometry and field. Investigations are being carried out to determine whether the optimizer routines from both packages yield the same solutions, given the same starting point. The work on the double-helix configuration has just begun. As illustrated in figure 10, a basic model capable of being used with the VF optimizer has been built and is ready to run.

In parallel, CCLRC/RAL has started the development of a 2D mechanical model of the NED Reference Design V1 based on ANSYS®. The model is in two steps. The first step includes the coil assembly, the ground plane insulation, pairs of austenitic steel collars and keys. It is used to simulate the collaring process during which the collars are implemented around the insulated coil assembly and are clamped by means of the keys to pre-compress the coil azimuthally. The second step includes the aforementioned collared-coil assembly completed by a two-piece, horizontally split, iron yoke and a welded outer shell that holds the coldmass together. The two yoke halves are assembled around the

[17] Vector Fields, 24 Bankside, Kidlington, Oxon OX5 1JE, United Kingdom.

Table 10. Salient material properties used by NED/WGMDO partners for mechanical computations.

Material	Used on	Elastic modulus (GPa) 4.2 K	Elastic modulus (GPa) 293 K	Poisson's ratio	Integrated thermal expansion (293–4.2 K)
Insulated and impregnated Nb_3Sn conductor stack	Coil	42	30	0.3	3.9×10^{-3}
Cu–Al alloy	Wedges/Spacers		110	0.3	-3.6×10^{-3}
G10	Spacer				
Fibre direction			28	0.3	-2.6×10^{-3}
Through thickness			6.4		-8.0×10^{-3}
Polyimide	Ground plane insulation		2.5	0.34	-6.0×10^{-3}
Austenitic stainless steel	Collar/ outer shell		194	0.3	-2.6×10^{-3}
Magnetic steel	Yoke		205	0.3	-2.1×10^{-3}

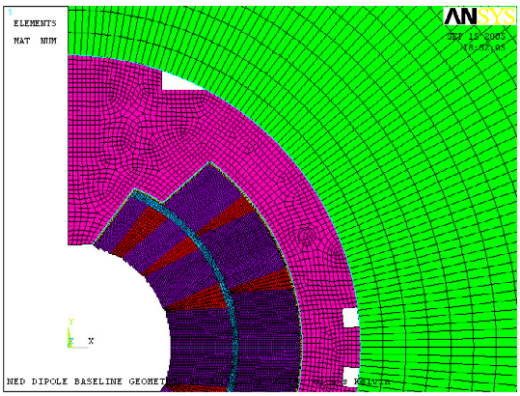

Figure 11. 2D mesh of the NED Reference Design V1 generated by CCLRC/RAL for mechanical computations (from inside outwards: conductor stack and Cu–Al alloy wedges, G10 interlayer spacer, polyimide ground plane insulation, stainless steel and iron yoke. The stainless steel outer shell surrounding the iron yoke is not visible here).

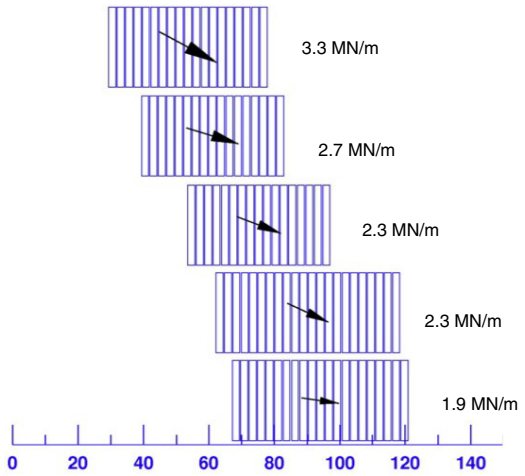

Figure 12. Conductor and Lorentz force distributions in the top right quadrant of 130 mm aperture, ellipse-type design developed by CEA.

collared-coil assembly in such way that there remains a gap at their midplane. The room-temperature coil pre-compression after collaring and the yoke midplane gap after shell welding must be optimized to ensure that, when the magnet is cold and energized, the coil remains under compression and the yoke midplane gap is closed, thereby providing a very stiff support against the Lorentz force. The first step of the model is now fully operational, while the details of the second step are being worked out. Figure 11 presents an overview of the coldmass mesh.

5.3. CEA contribution

CEA has been working on an original design referred to as *ellipse-type*, and has carried out 2D electromagnetic analyses of 88, 130 and 160 mm aperture models using ROXIE. It has been shown that, in each case, accelerator-field quality can be reached by optimizing the conductor distribution and that the peak-to-central-field ratio is very advantageous. Nevertheless, the Lorentz forces involved are huge a lot of attention has to be paid to the mechanical design. CEA is presently developing a mechanical model of the 130 mm aperture design based on CASTEM[18]. As an illustration, figure 12 presents the conductor and Lorentz force distributions for the 130 mm aperture design.

In parallel, and at the margin of the WGMDO efforts, CEA has been subcontracted by EFDA to study a 130 mm aperture, 12.5-central-field, dipole magnet relying on a conventional $\cos\theta$, layer design. The preliminary mechanical analysis carried out as part of this study concludes that the Lorentz stresses originating in the coils are excessive and that there is no easy way to control and limit them [36]. This may indicate that such a field level in such an aperture is out of reach for the conventional $\cos\theta$, layer design and that one needs to rely on a different magnetic configuration.

5.4. CERN contribution

CERN has pursued the 2D electromagnetic optimization of Reference Design V1 with ROXIE. The optimization was carried out with respect to

[18] CASTEM is a trademark from CEA/Saclay France.

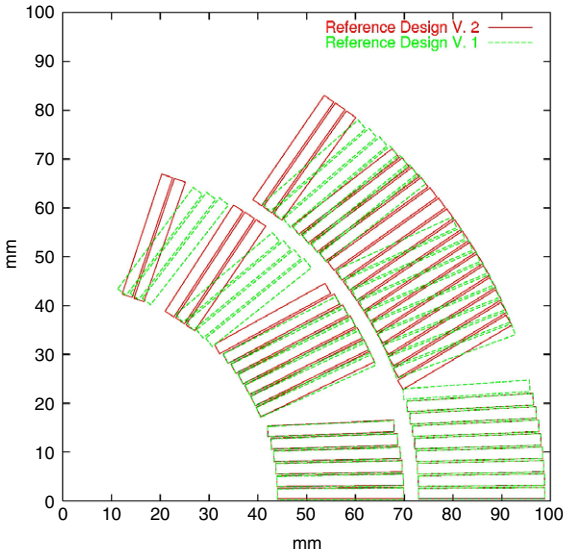

Figure 13. Comparison of conductor distributions for the NED Reference Designs V1 (dashed lines) and V2 (continuous lines) after re-optimization at CERN.

- conductor geometry (to minimize all multipole coefficients and improve radial positioning of conductor blocks in 2D cross-section),
- the shape of the iron yoke inner boundary (to minimize saturation effects),
- the size and implementation of ferromagnetic shims (to compensate superconductor magnetization effects).

The re-optimization has now been completed and has led to the definition of a new reference design, referred to as Reference Design V2, with a good field quality (all multipole coefficients are below 1 unit at a reference radius of 29 mm, save for the normal 18-pole, b_9, which is equal to 1.7 unit and the normal 22-pole, b_{11}, which is equal to 2.7 unit), efficient peak-to-central-field ratio (∼1.03–1), 15.0 T conductor peak field for a quench current of 29.4 kA and a more radial conductor distribution. Figure 13 presents a comparison of the two reference designs.

Regarding iron saturation, figure 14(a) presents a comparison of the distortions of the normal sextupole coefficient, b_3, computed for the conductor distribution of Reference Design V2 and two different yoke configurations: one with a circular inner boundary (with an inner radius of 125.4 mm) and one with an optimized, elliptical inner boundary (with a vertical, half major axis of 136.6 mm and an horizontal, half minor axis of 125.4 mm). Relying on an elliptical inner boundary enables one to reduce the b_3 peak-to-peak variations by a factor ∼3. Let us recall that the effects of iron saturation on the field quality of $\cos\theta$ magnets have been identified for more than 30 years [37] and that the idea of shaping the iron yoke to compensate them has been around for almost as long [38]. To the authors' knowledge, the first systematic study on a yoke with an elliptical inner boundary was carried out within the framework of the relativistic heavy ion collider (RHIC) project at BNL in the mid-1980s [39].

Regarding superconductor magnetization, figure 14(b) presents a comparison of the induced b_3 hystereses computed

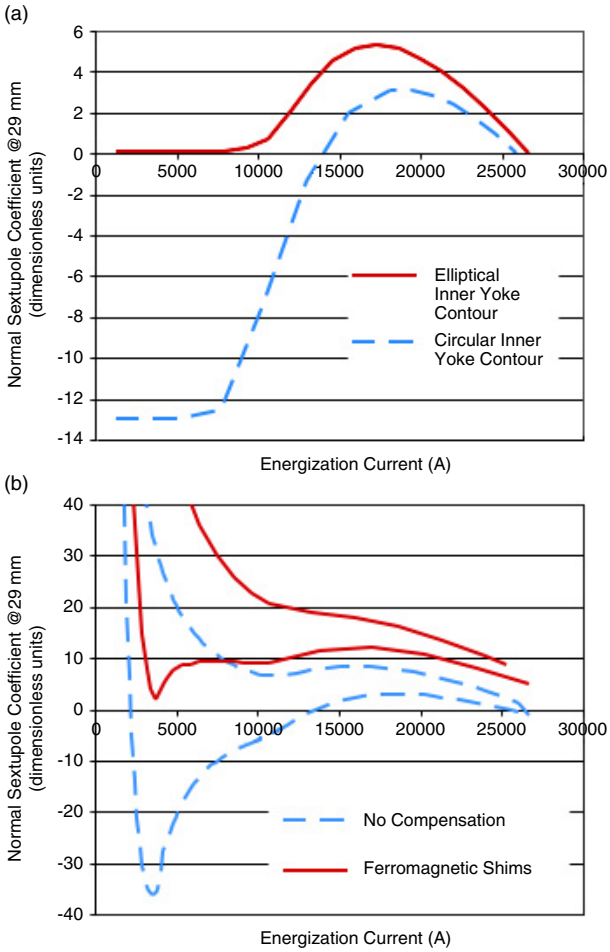

Figure 14. Results of feasibility studies carried out at CERN to reduce the distortions of normal sextupole coefficient, b_3: (a) comparison of saturation effects produced by an iron yoke with a circular inner boundary (dashed line) and with an optimized elliptical inner boundary (continuous line; top) and (b) comparison of hystereses produced by superconductor magnetization (extrapolated to a conductor with a non-Cu J_C of 3000 A mm^{-2} and an effective outer filament diameter of 50 μm) without corrective shims (dashed line) and with two optimized ferromagnetic shims astutely implemented in the coil cross-section (continuous line; bottom).

when taking into account the full effect (no corrective shims) and when introducing two ferromagnetic shims at suitable locations inside the coils: one 1.5 mm thick shim attached right below the upper wedge of the outer layer and one 0.7 mm thick shim attached right below the middle wedge of the inner layer, as shown in figure 15. The effects of persistent magnetization currents were estimated using a ROXIE feature which combines a vector hysteresis model for hard superconductors with the BEM–FEM method and which relies on a given $J_C(B)$ fit function for the superconducting filaments [40]. The $J_C(B)$ function used in the simulation is shown in figure 16. It was extracted from magnetization measurements performed by Twente University on an existing 0.9 mm diameter, 504-filament PIT wire produced by SMI in 2000 [41], appropriately rescaled to the NED specifications (in particular, with respect to the non-copper critical current density of 3000 A mm^{-2} at 4.2 K and 12 T and to the effective filament outer diameter of 50 μm). The introduction

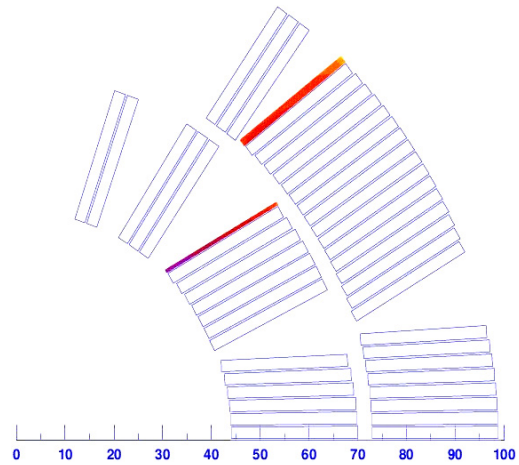

Figure 15. Implementation of corrective ferromagnetic shims to compensate the effects of persistent magnetization currents in the NED Reference Design V2 optimized by CERN.

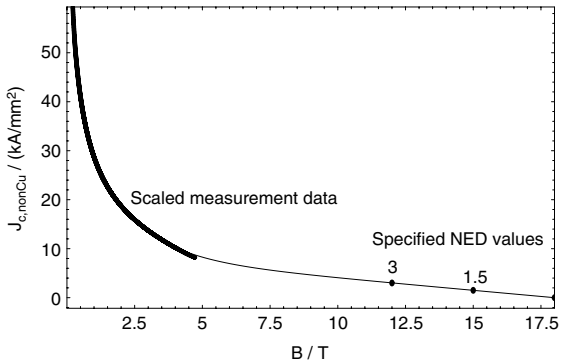

Figure 16. Extrapolated, non-copper critical current density, J_C, versus magnetic flux density, B, curve used by CERN to compute persistent magnetization current effects in the NED.

of the two ferromagnetic shims enables one to reduce the b_3 variations during the up-ramp (lower part of the hysteresis curves) by a factor in excess of 3. As for iron saturation, the effects of superconductor magnetization have been known for more than 30 years [42]. The idea of compensating them by ferromagnetic shims was first proposed at the time of Superconducting Super Collider (SSC) project [43] and was revived in the late 1990s when it became clear that the effective filament diameters of Nb_3Sn wires would remain significantly higher than those achieved in Nb–Ti wires. At the time, LBNL suggested a thin, continuous, iron coating on the magnet bore tube [44] while FNAL investigated segmented ferromagnetic strips distributed around the magnet bore tube and a ferromagnetic cable core [45]. The idea of using simple but very effective shims attached to the coil wedges was first discussed in [46].

The encouraging results of figures 14(a) and (b) show that the selected correction schemes can be quite effective (at least on the normal sextupole coefficient, b_3), and that we do have some means of compensating the effects of both iron saturation and superconductor magnetization.

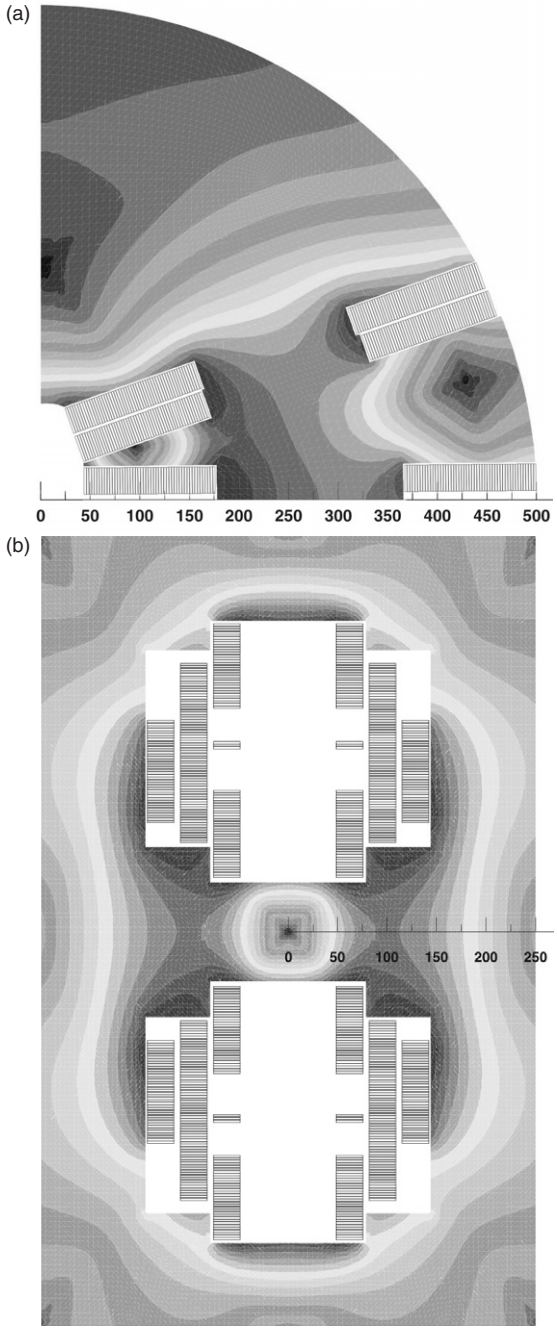

Figure 17. Examples of 2D, 88 mm aperture, electromagnetic designs investigated by CIEMAT: (a) motor-type (top) and (b) common-coil (bottom).

5.5. CIEMAT contribution

CIEMAT has worked on the 2D electromagnetic analysis of the 88 and 130 mm aperture motor-type design and of the 88 mm aperture common-coil design using ROXIE. Starting from the set of design parameters agreed upon by the working group, the field quality has been optimized in the cross-section while keeping an eye on the feasibility of the mechanical design and on the Lorentz forces to be handled. For both configurations, the number of design variables is enough to get an optimum field quality, as well as a good peak-to-central-field ratio.

However, the motor-type design appears to yield a high fringe field while calling for a large superconductor volume. As an illustration, figures 17(a) and (b) show examples of the 88 mm aperture motor-type and common coil designs investigated by CIEMAT.

6. Conclusion

Save for the innovative insulation, all the tasks of the NED Activity have been launched and are well under way. The cryostat for heat transfer measurements has been completed and it was delivered to CEA/Saclay on 20 September 2005, where it is being readied for commissioning. The next few months will be critical for the conductor development task, with the results of STEP1 wires. Polyimide-sized glass fibre tapes seem a promising alternative to conventional insulation systems. The NED collaborators remain of course eager to achieve their initial goals and are still actively seeking additional funding to complete the detailed design, manufacture and test of the model magnet left out from the CARE contract.

Acknowledgments

The authors wish to thank Roy Aleksan and Lucio Rossi for their continuous and active support. This work was supported in part by the European Community–Research Infrastructure Activity under the FP6 'Structuring the European Research Area' programme (CARE, contract number RII3-CT-2003-506395).

References

[1] Napoly O *et al* 2005 The CARE accelerator R&D programme in Europe *2005 Particle Accelerator Conf. (Knoxville, TN, May)*
[2] Devred A *et al* 2004 High field accelerator magnet R&D in Europe *IEEE Trans. Appl. Supercond.* **14** 339–44
[3] Devred A 2005 Status of the Next European Dipole (NED) activity of the Coordinated Accelerator Research in Europe (CARE) project *IEEE Trans. Appl. Supercond.* **15** 1106–12
[4] Strait J *et al* 2003 Towards a new LHC interaction region design for a luminosity upgrade *Proc. 2003 Particle Accelerator Conf.* pp 42–4
[5] Devred A 2003 High field accelerator magnets beyond LHC *Proc. 2003 Particle Accelerator Conf.* pp 146–50
[6] Devred A, Gourlay S and Yamamoto A 2005 Future accelerator magnet needs *IEEE Trans. Appl. Supercond.* **15** 1192–9
[7] Gourlay S A *et al* 2005 Magnet R&D for the US LHC Accelerator Research Program (LARP) *19th Int. Conf. on Magnet Technology (Genova, Italy, Sept. 2005)*
[8] Zlobin A V *et al* 2005 R&D of Nb_3Sn accelerator magnets at Fermilab *IEEE Trans. Appl. Supercond.* **15** 1113–8
[9] Lietzke A F *et al* 2005 Test results of HD1b, an upgraded 16 tesla Nb_3Sn dipole magnet *IEEE Trans. Appl. Supercond.* **15** 1123–7
[10] http://lt.tnw.utwente.nl/project.php?projectid=9
[11] Burnod L *et al* 1994 Thermal modelling of the LHC dipoles functioning in superfluid helium *Proc. 1994 European Particle Accelerator Conf.* pp 2295–7
[12] Meuris C *et al* 1999 Heat transfer in electrical insulation of LHC cables cooled with superfluid helium *Cryogenics* **39** 921–31
[13] Zlobin A V *et al* 2003 Conceptual design study of Nb_3Sn low-beta quadrupoles for 2nd generation LHC IRs *IEEE Trans. Appl. Supercond.* **13** 1266–9
[14] Rossi L and Sorbi M 2004 *QLASA: A Computer Code for Quench Simulation in Adiabatic Multicoil Superconducting Windings* INFN/TC-04/13 http://www.lnf.infn.it/sis/preprint/pdf/INFN-TC-04-13.pdf
[15] MAST and SABER® are commercialized by Synopsis, Inc. 700 East Middlefield Road Mountain View, CA 94043, USA http://www.synopsys.com/products/mixedsignal/saber/saber.html
[16] Hagedorn D and Rodriguez-Mateos F 1992 Modelling of the quenching process in complex superconducting magnet systems *IEEE Trans. Magn.* **28** 366–9
[17] Granata V *et al* 2005 Study of the protection of system for cos-theta NED dipole *19th Int. Conf. on Magnet Technology (Genova, Italy, Sept. 2005)*
[18] Russenschuck S 2005 *Electromagnetic Design and Mathematical Optimization Methods in Magnet Technology* E-book 2nd edn (Geneva, Switzerland: CERN) ISBN: 92-9083-242-8 http://russ.home.cern.ch/russ
[19] Patoux A, Pérot J and Rifflet J M 1983 Test of new accelerator superconducting dipoles suitable for high precision field *IEEE Trans. Nucl. Sci.* **30** 3681–3
[20] Wada H *et al* 1994 VAMAS intercomparison of critical current measurements on Nb_3Sn superconductors: a summary report *Cryogenics* **34** 899–908
[21] Goodrich L F and Srivastava A N 1994 A simple and repeatable technique for measuring the critical current of Nb_3Sn wires *Proc. 7th Int. Workshop on Critical Currents in Superconductors* pp 609–12
[22] Den Ouden A *et al* 2005 Critical current measurements on Nb_3Sn conductors for the NED project *19th Int. Conf. on Magnet Technology (Genova, Italy, Sept. 2005)*
[23] Greco M *et al* 2005 Magnetization measurements of Nb_3Sn wires for the Next European Dipole (NED) *19th Int. Conf. on Magnet Technology (Genova, Italy, Sept. 2005)*
[24] Durante M *et al* 2001 Development of a Nb_3Sn multifilamentary wire for accelerator magnet applications *Physica* C **354** 449–53
[25] Devred A 2002 Insulation systems for Nb_3Sn accelerator magnet coils manufactured by the wind and react technique *IEEE Trans. Appl. Supercond.* **12** 1232–7
[26] Canfer S J, Baynham D E and Greenhalgh R J S 2005 Insulation development for the Next European Dipole *2005 Cryogenic Engineering Conf./Int. Cryogenic Materials Conf. (Keystone, CO, Aug. 29–Sept. 2 2005)*
[27] Puigségur A *et al* 2003 Development of an innovative insulation for Nb_3Sn wind and react coils *Adv. Cryo. Eng. (Mater.)* **50** 266–72
[28] Quettier L *et al* 2005 An innovative insulation for Nb_3Sn wind and react coils: electrical tests *19th Int. Conf. on Magnet Technology (Genova, Italy, Sept. 2005)*
[29] Leroy D *et al* 1998 Design features and performance of a 10 T twin aperture model dipole for LHC *Proc. 15th Int. Conf. on Magnet Technology* (Beijing: Science Press) pp 119–22
[30] Leroy D *et al* 2000 Design and manufacture of a large-bore 10 T superconducting dipole for the CERN cable test facility *IEEE Trans. Appl. Supercond.* **10** 178–82
[31] den Ouden A *et al* 1994 An experimental 11.5 T Nb_3Sn LHC type of dipole magnet *IEEE Trans. Magn.* **30** 2320–3
[32] Dell'Orco D, Scanlan R M and Taylor C E 1993 Design of the Nb_3Sn dipole D20 *IEEE Trans. Appl. Supercond.* **3** 82–6
[33] Danby R G *et al* 1983 Panel discussion of magnets for a big machine *Proc. 12th Int. Conf. on High-Energy Accelerators* pp 52–62
[34] Gupta R C 1998 A common coil design for high field 2-in-1 accelerator magnets *Proc. 1997 Particle Accelerator Conf.* pp 3344–6
[35] Meyer D I and Flask R 1970 A new configuration for a dipole magnet for use in high energy physics applications *Nucl. Instrum. Methods* **80** 339–41

[36] Portone A and Salpietro E 2005 Conceptual design of the 12.5 T superconducting EFDA dipole *19th Int. Conf. on Magnet Technology (Genova, Italy, Sept. 2005)*
[37] Parzen G and Jelett k 1971 Saturation effects in high-field superconducting magnets *IEEE Trans. Nucl. Sci.* **18** 646–8
[38] Coupland J H, Simkin J and Randle T C 1973 Very high field synchrotron magnets with iron yokes *Nucl. Instrum. Methods* **106** 595–604
[39] Morgan G 1985 Use of an elliptical aperture to control saturation in closely coupled, cold iron, superconducting dipole magnets *IEEE Trans. Nucl. Sci.* **32** 3695–7
[40] Aleksa M *et al* 2004 A vector hysteresis model for superconducting filament magnetization in accelerator magnets *IEEE Trans. Magn.* **40** 864–7
[41] den Ouden A *et al* 2001 Progress in the development of an 88 mm Bore 10 T Nb_3Sn dipole magnet *IEEE Trans. Appl. Supercond.* **11** 2268–71
[42] Green M A 1971 Residual field in superconducting dipole and quadrupole magnets *IEEE Trans. Nucl. Sci.* **18** 664–8
[43] Green M A 1987 Control of the fields due to superconductor magnetization in the SSC magnets *IEEE Trans. Magn.* **23** 506–9
[44] Caspi S 1999 private communication
[45] Kashikin V V and Zlobin A V 2001 Correction of the persistent current effect in Nb_3Sn dipole magnets *IEEE Trans. Appl. Supercond.* **11** 2058–61
[46] Kashikin V V, Barzi E *et al* 2003 Passive correction of the persistent current effect in Na_3Sn dipole magnets *IEEE Trans. Appl. Supercond.* **13** 1270–3